

‡Supported by the National Science Foundation and the U. S. Office of Naval Research.

¹H. Bethe, *Am. Physik* **71**, 205 (1931); see also L. Hulthén, *Arkiv Met. Astron. Fysik* **26A**, 11 (1938).

²M. T. Hutchings, G. Shirane, R. J. Birgeneau, and S. L. Holt, *Phys. Rev. B* **5**, 1999 (1972).

³M. E. Fisher, *Am. J. Phys.* **32**, 343 (1964).

⁴P. M. Richards, *Phys. Rev. Letters* **28**, 1646 (1972).

⁵*N*-methyl phenazinium tetracyanoquinodimethan. For a review of the molecular physics and solid-state properties see Ref. 7.

⁶C. J. Fritchie, Jr., *Acta Cryst.* **20**, 892 (1966).

⁷A. J. Epstein, S. Etamad, A. F. Garito, and A. J. Heeger, *Phys. Rev. B* **5**, 952 (1972).

⁸E. Ehrenfreund, E. F. Rybaczewski, A. F. Garito, and A. J. Heeger, *Phys. Rev. Letters* **28**, 873 (1972). The dipolar coupling is small (a few percent) compared to the isotropic hyperfine interaction.

⁹This mechanism, which is unimportant in 3D systems because of the negligible state density near $q=0$, gives a contribution to T_1^{-1} proportional to $k_B T(1 + \omega^2 \tau_1^2)^{-1}$, where τ_1 is the *electronic* longitudinal relaxation time, and thus is experimentally unimportant above a few kilogauss and does not affect the rate at $T \rightarrow 0$ °K.

¹⁰L. N. Bulaevsii, *Zh. Eksperim. i Teor. Fiz.* **43**, 968 (1962) [*Sov. Phys. JETP* **16**, 685 (1963)].

¹¹C. P. Slichter, *Principles of Magnetic Resonance* (Harper & Row, New York, 1963), p. 120.

¹²T. Moriya, *Progr. Theoret. Phys. (Kyoto)* **16**, 23 (1956).

¹³J. C. Bonner and M. E. Fisher, *Phys. Rev.* **135**, A640 (1964).

¹⁴D. Beeman and P. Pincus, *Phys. Rev.* **166**, 359 (1968).

¹⁵J. des Cloizeaux and J. J. Pearson, *Phys. Rev.* **128**, 2131 (1962).

PHYSICAL REVIEW B

VOLUME 7, NUMBER 1

1 JANUARY 1973

Lead Centers in Cesium Halides

S. Radhakrishna and K. P. Pande

Department of Physics, Indian Institute of Technology, Madras-36, India

(Received 29 March 1972; revised manuscript received 1 June 1972)

Lead as an impurity in cesium halides gives the usual *A*, *B*, and *C* bands with some differences, such as the appearance of a doublet structure in the *A* band and the observation of an aggregate lead complex band in the visible region, when compared with the results for the other lead-doped alkali halides. In this paper the peak positions, half-widths, and dipole-strength ratios of these lead centers in CsCl, CsBr, and CsI are reported. In irradiated cesium halides containing divalent lead, a new band is observed in the uv region at about 20 nm to the shorter-wavelength side of the *A* band. This band is interpreted to be due to Pb^+ from various optical absorption studies and is found to be stable up to 110 °C. In crystals irradiated for a longer time, this Pb^+ band goes down along with the Pb^{2+} bands and a new band is observed which is attributed to Pb^0 . It has been found from conductivity studies that the binding energy for an impurity-vacancy pair in cesium halides is about 0.48 eV and the presence of divalent lead in these crystals decreases the conductivity in the extrinsic region. From the dielectric-loss measurements, the migration energy for a cation vacancy bound to the impurity is found to be ~ 0.62 eV while the preexponential factor is of the order of $3 \times 10^{10} \text{ sec}^{-1}$.

I. INTRODUCTION

A considerable amount of work has been published¹⁻⁶ on the nature and properties of defect centers in lead-doped sodium and potassium halides (fcc structure), but no data are available on lead-doped cesium halides (bcc structure). Optical absorption studies⁷ of Tl^+ (another ion of the s^2 family) in cesium halides have revealed some new features such as different temperature behavior of the *B* band and six, instead of the usual four, bands in alkali halides containing such impurities. Hence, it was thought desirable to undertake a study of the behavior of lead centers in such bcc structures by optical absorption, radiation damage, electrical conductivity, and dielectric-loss techniques. The electrical conductivity of cesium

halides has been investigated previously⁸⁻¹⁰ but the association region has not been found. It has also been established⁸ that anion vacancies are more mobile than cation vacancies. The dielectric-loss studies in bcc structures containing charge-compensating defects have not been studied so far and the results pertaining to the dielectric-loss measurements of the lead-impurity-vacancy dipole in cesium halides are presented in this paper.

II. EXPERIMENTAL METHODS

Some single crystals of pure cesium halides have been obtained from other research groups, while some pure and lead-doped crystals were grown in our laboratory by the Bridgman technique. Lead was diffused into pure crystals by heating the lead metal and cesium halide crystals together in an

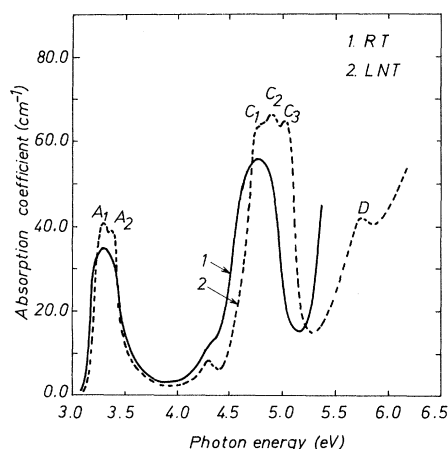


FIG. 1. Optical absorption spectrum of CsI crystal containing 100 ppm of lead, at RT (curve 1) and LNT (curve 2).

evacuated Pyrex glass tube at 500 °C for about 36 h. By controlling the temperature and the time of heating, the amount of lead present in the crystals can be controlled. The impurity content estimated from mass spectrometry and the atomic absorption spectroscopy technique was found to be typically of the order of 100 ppm. Optical absorption studies were made at different temperatures on the Cary-14 spectrophotometer and the radiation damage was effected by a Philips x-ray unit operating at 35 kV and 15 mA. Electrical conductivity measurements were made in the temperature range 100–450 °C by heating the sample in a furnace and measuring the resistance by a GR 1644-A bridge. A thin coating of aquadag was applied to the opposite faces of the crystal, and the crystal was put between two plates made of an alloy of platinum-rhodium. The temperature of the crystal was recorded by a copper-constantan thermocouple. The resistance was measured across 100 V applied to the crystal faces after allowing it to stabilize at the desired temperature. Dielectric-loss measurements at different temperatures were made by using a GR 1615-A capacitance bridge combined with a GR 1311-A audio oscillator. For a large range of the frequency a PM 5100 Philips oscillator was used in combination with the capacitance bridge. Just before making the dielectric-loss measurements the crystal was quenched from 300 °C to room temperature after keeping the crystal at 300 °C for 2 h. The crystal was painted on opposite faces with aquadag colloidal graphite paste and was heated in a vacuum in a sample holder similar to one described previously.¹¹ The temperature of the crystal was kept constant at any desired value by using a plastomatic Philips temperature controller.

III. RESULTS AND DISCUSSION

A. Optical Absorption

1. Uncolored Crystals

The absorption bands observed in alkali halides containing impurities with ns^2 configuration have been classified^{2,12} as the A, B, C, and D bands, in order of decreasing wavelengths. The transitions responsible for these bands are

$$A \text{ band: } {}^1A_{1g} \rightarrow {}^3T_{1u} \quad ({}^1S_0 \rightarrow {}^3P_1),$$

$$B \text{ band: } {}^1A_{1g} \rightarrow {}^3T_{2u} \text{ or } {}^3E_u \quad ({}^1S_0 \rightarrow {}^3P_2),$$

$$C \text{ band: } {}^1A_{1g} \rightarrow {}^1T_{1u} \quad ({}^1S_0 \rightarrow {}^1P_1).$$

Since the singlet-triplet transition is not consistent with the spin selection rule, the C band should be stronger than the A band; this has been confirmed experimentally. The transition assigned to the B band is forbidden, but this band appears with a small intensity because of thermal lattice vibrations. The A and C bands are also known to exhibit structure under certain temperature conditions.

Figure 1 shows the optical absorption spectrum of lead-doped CsI crystal measured at room temperature (curve 1) and liquid-nitrogen temperature (curve 2). These curves have been obtained after subtracting the background absorption which is very much temperature sensitive. A, B, and C bands have been observed both at room temperatures (RT) and liquid-nitrogen temperature (LNT), whereas the D band could be observed only at LNT. The height of A and C bands increases, and their peak positions shift to the higher-energy side as the temperature is lowered. The structure in these bands is very clear at LNT. The intensity of the B band is found to be lower at LNT as compared to that at RT, indicating that the transition responsible for this band is vibronically induced, just as in the case of the other lead-doped alkali halides. Figure 2 represents the temperature variation of the C

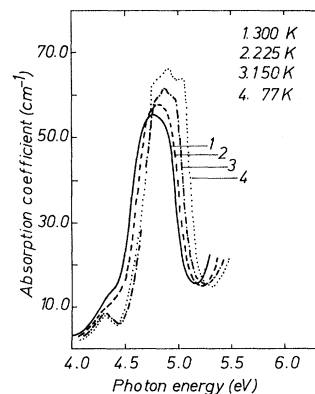


FIG. 2. Temperature variation of C band in lead-doped CsI crystal. Curves 1, 2, 3, and 4 represent the spectrum taken at 300, 225, 150, and 77 K, respectively.

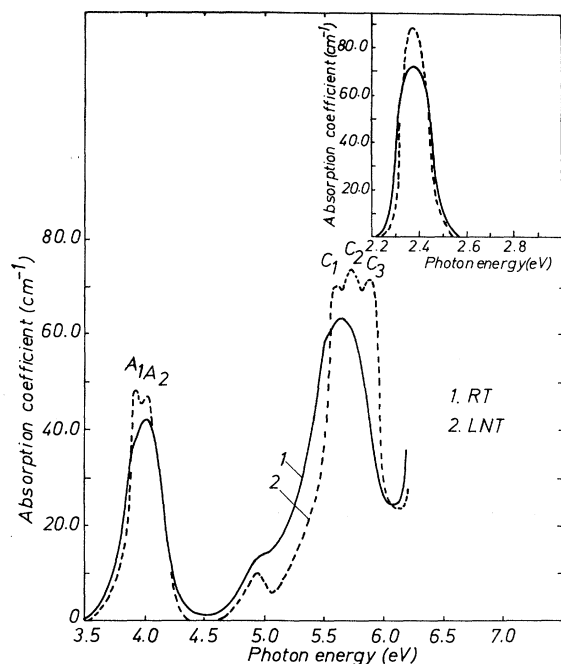


FIG. 3. Optical absorption spectrum of CsBr crystal containing 100 ppm of lead. Curves 1 and 2 represent the spectrum taken at RT and LNT, respectively.

band. It can be seen that as the temperature increases the structure in the *A* and *C* bands becomes asymmetric and the separation between the component bands increases. The half-widths of the *C* and *B* bands are found to vary linearly with temperature. Figure 3 shows similar optical absorption results for lead-doped CsBr crystal. Comparison of the structure of the *A* and *C* bands in CsI and CsBr indicates that the structure is better resolved in CsBr. This might indicate that the mass of halogen ions might be playing a prominent role in determining the separation between the components in the *A* and *C* bands. The important feature in CsBr doped with lead is that if the crystal is not quenched before taking the measurements, an intense band appears at 2.38 eV with a half-width of 0.16 eV. At LNT this band becomes sharp and the half-width reduces to 0.10 eV, but it exhibits no structure. This band is observed in the crystal in which the impurity has been introduced by diffusion mechanism. If such a crystal is quenched from higher temperature ($\sim 400^\circ\text{C}$), the band gradually reduces in intensity and finally disappears, indicating that this is due to an aggregated lead complex which dissolves when the crystal is quenched from high temperatures. Such behavior is found only if lead is diffused for longer periods of time (more than 12 h). Similar behavior is observed in CsCl, where the band peaks at 2.46 eV with half-widths of 0.17 eV at RT and 0.11 eV at

LNT.

In order to calculate the half-widths and the dipole-strength ratios, the observed bands were analyzed by a curve-fitting method. It was assumed that each absorption band approximates to a Gaussian curve with an equation

$$D = D_0 \exp[-4 \log_{10} 2 / H^2 (E - E_0)^2], \quad (1)$$

where D and D_0 refer to the optical densities corresponding to the band energies E and E_0 , respectively; E_0 is the band maxima in eV. H is the half-width of the bands, which is varied to obtain a best fit for the experimental curves. The values of D for different values of E were computed on a Hewlett-Packard calculator model 9100-A. The results regarding the peak positions and half-widths of the Pb^{++} bands in cesium halides obtained from the optical absorption studies are summarized in Table I.

Various suggestions¹³⁻¹⁵ have been given to explain the structure exhibited by the *A* and *C* bands; among these only the dynamical Jahn-Teller effect seems to explain the observed facts. In the present experiment the observed increase in the asymmetry and splitting between the component bands with temperature also suggests that the dynamical Jahn-Teller effect is the underlying cause of the observed structure. In accordance with earlier explanations,¹⁵ the vibrational modes E_g (tetragonal) and T_{2g} (trigonal), which exist in the vibrational modes of a quasimolecule composed of lead ion and surrounding anions, have linear interaction with the optically allowed triply degenerate excited state T_{1u} of the lead ion. These vibrational modes cause the deformation of the octahedron formed by the anions around the activator ion. Essentially, the extra charge of the lead ion will draw the nearest-neighbor halide ions closer and repel the next-nearest-neighbor cesium ions, which will make the T_{2g} distortion easier. Thus linear interaction between T_{2g} mode and T_{1u} state is mainly responsible for the instantaneous splitting in the excited state which appears as a structure in the optical absorption bands, although the effect of E_g mode is also appreciable. In the present investigation the *A* band shows only a doublet structure instead of the expected triplet, probably because two components in the *A* band might have coalesced into one, thus giving rise to the doublet structure. The quadratic interaction between the *A* and *B* bands through T_{2g} lattice vibrations might be responsible for the coalescence of two components in the *A* band.

The T_{2g} and E_g modes of vibrations probably mix the forbidden and allowed states, giving rise to the vibration-induced transition responsible for the *B* band, with intensity proportional to absolute temperature. In the present investigation it has been confirmed (as will be discussed later) that for lead-

TABLE I. Peak positions (eV) and half-widths (eV) of Pb²⁺ bands in cesium halides at room temperature (RT) and liquid-nitrogen temperature (LNT).

Crystals		RT			LNT						
		A	B	C	A ₁	A ₂	B	C ₁	C ₂	C ₃	D
CsCl: Pb ²⁺	Peak position	4.46	5.28	6.20	4.35	4.48	5.34	6.08	6.20	6.32	...
	Half-width	0.34	0.27	0.57	0.16	0.15	0.26	0.18	0.17	0.17	...
CsBr: Pb ²⁺	Peak position	4.00	4.92	5.64	3.92	4.01	4.94	5.58	5.74	5.90	...
	Half-width	0.32	0.24	0.54	0.14	0.13	0.22	0.17	0.17	0.16	...
CsI: Pb ²⁺	Peak position	3.32	4.27	4.79	3.38	3.33	4.30	4.77	4.90	5.04	5.77
	Half-width	0.29	0.20	0.50	0.12	0.11	0.14	0.16	0.15	0.14	0.48

doped cesium halides, the *B* band borrows intensity from the *C* band.

In order to get an idea whether the excited state for the *B* band is closer to that of the *C* or *A* bands, dipole-strength ratios have been calculated by using Sugano's¹⁶ formula

$$R_{\text{Sug}} = \frac{4 - 2x + [6 - 2(2x - 1)^2]^{1/2}}{2 + 2x - [6 - 2(2x - 1)^2]^{1/2}}, \quad (2)$$

where

$$x = (E_B - E_A)/(E_C - E_A).$$

E_A , E_B , and E_C are the observed band positions of the *A*, *B*, and *C* bands expressed in eV, respectively. Thus one can calculate the value of R_{Sug} , i. e., the dipole-strength ratio from the observed peak positions of the *A*, *B*, and *C* bands. This ratio can also be calculated from oscillator strengths of the observed bands by using the formula

$$R_{\text{obs}} = (f_C/f_A)(E_A/E_C), \quad (3)$$

where f_C and f_A are the oscillator strengths of the

C and *A* bands, respectively. However since the data on refractive indices (at different wavelengths) for cesium halides are not complete, we were unable to calculate the oscillator strengths. As there is not much difference between R_{Sug} and R_{obs} in other alkali halides² containing lead, we can get a fairly good idea about the value of R . Table II summarizes our data for R and compares them with other alkali halides doped with lead.

According to the Sugano theory,¹⁶ if the excited state of the *B* band is nearer to that of the *C* band, then the value of R must be between 2.0 and 9.9; whereas, if it is nearer to the excited state of the *A* band, then the value should be larger than 9.9. In the present work, as is evident from Table II, the value of R is smaller than 9.9, and hence the excited state of the *B* band is closer to that of the *C* band. In other words, the closeness of the excited states of the *B* and *C* bands favors mixing, and therefore the appearance of the *B* band. The peak positions of the *A*, *B*, and *C* bands plotted as a function of the interionic distance, give three corresponding straight lines, thus indicating that a Mollwo-Ivey relation of the type¹⁷ $E = KR^n$ can be

TABLE II. Comparison of dipole-strength ratios between alkali halides (fcc structure) and cesium halide (bcc structure).

Crystal	E_A	E_B	E_C	$X = \frac{E_B - E_A}{E_C - E_A}$	R_{Sug}	R_{obs}	Ref.
Free Pb ²⁺	7.983	9.792	11.820	0.471	11.2	...	2
NaCl: Pb ²⁺	4.550	5.910	6.250	0.800	3.60	3.2	2
KCl: Pb ²⁺	4.570	5.860	6.230	0.777	3.80	4.2	2
CsCl: Pb ²⁺	4.459	5.275	6.198	0.510	10.54	...	This work
CsBr: Pb ²⁺	3.999	4.919	5.635	0.562	7.81	...	This work
CsI: Pb ²⁺	3.314	4.274	4.786	0.652	5.72	...	This work

TABLE III. Values of constants n and K of $M-I$ type relation for cesium halides containing divalent lead.

Bands	n	K
A	-1.50	27.35
B	-1.13	20.05
C	-1.30	28.25

found. The relevant parameters are given in Table III.

2. Colored Crystals

The effect of radiation damage in CsBr containing 100 ppm of lead is shown in Fig. 4, where curves 1, 2, 3, and 4 represent the spectra of the lead-doped crystal irradiated for different lengths of time. It can be seen from curves 2 and 3 that as irradiation continues, the Pb^{2+} bands reduce in intensity and a new band at 4.22 eV starts appearing. The reduction in the intensity of Pb^{2+} bands indicates that some charge conversion takes place during irradiation. Recently⁶ electron paramagnetic resonance (EPR) due to Pb^{3+} ions in KCl crystals, formed on irradiating the crystal at LNT and then warming it up to 273 K, has been reported. However in the present investigation no EPR signal other than that of the F centers (not shown in Fig. 4) could be detected, even if measurement is made at LNT, while irradiation is done at RT. Therefore, the possibility of the formation of Pb^{3+} seems remote. Further, three optical bands were found⁶ to be associated with the Pb^{3+} centers, while we found only one band (at 4.22 eV) appearing after

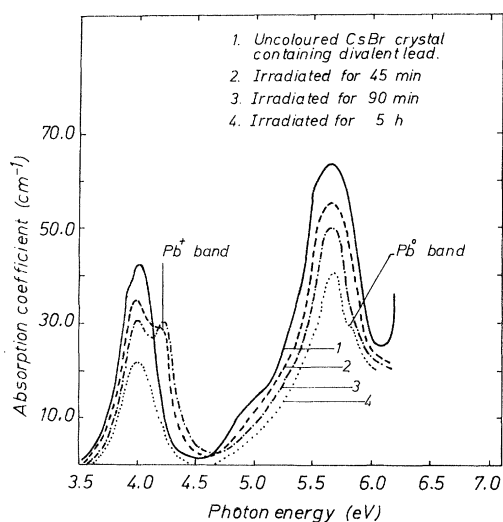


FIG. 4. Results of radiation damage in CsBr crystal containing lead. Curve 1 is for an uncolored lead-doped CsBr crystal. Curves 2, 3, and 4 are obtained for the irradiation time of 45, 90, and 300 min, respectively.

radiation damage. Thus, it seems that the Pb^{2+} ion is converted to the monovalent state associated with a band at 4.22 eV on irradiation at RT (Table IV), which is in accordance with the earlier results^{18,19} for lead-doped alkali halides (fcc structure). This Pb^+ band has a half-width of 0.25 eV at RT, and on lowering the temperature (curve not shown in Fig. 4) this band becomes sharp. The intensity of this band increases up to an irradiation time of 90 min, beyond which it starts reducing again, showing thereby that Pb^+ starts converting to Pb^0 for longer irradiation time. In the case of long irradiation the large number of electrons provided readily convert Pb^{2+} to Pb^0 , obviously through Pb^+ . Thus the band observed at 5.82 eV (curve 4) can be ascribed to Pb^0 on the basis of its temperature dependence. The temperature dependence of the bands observed at 5.82 and 4.22 eV are very different, which indicates that they are due to different centers. While the band at 5.82 eV is stable up to 500 °C and above, the band at 4.22 eV is stable only up to 110 °C, beyond which it reduces rapidly. Efforts to obtain a paramagnetic signal due to such Pb^+ ions have not been successful possibly because of the large F band present in the crystal or the large spin-orbit coupling of the lead ions.

B. Transport Properties

1. Electrical Conductivity

Previous work²⁰ on conductivity measurements in alkali halides of NaCl structure has led to an adequate model for the defect nature in these salts, but detailed studies have not been made on the CsCl structure. It has been shown⁸⁻¹⁰ that Schottky defects are prominent defects in cesium halides, but in contrast to alkali halides (fcc structure), the anion vacancies are more mobile. Electrical conduction in doped cesium halides has been reported previously,^{9,10} but the results regarding the association region are not consistent. Therefore, in the present study, the conductivity in lead-doped cesium halides has been measured in the low-temperature region (100–450 °C) in order to get an idea about the binding energy for the impurity bound to the cesium vacancy.

Figure 5 shows the electrical conductivity results

TABLE IV. Peak positions and half-widths of Pb^+ band in cesium halides at room temperature (RT) and liquid-nitrogen temperature (LNT).

Crystal	Peak position (eV)		Half-width (eV)	
	RT	LNT	RT	LNT
CsCl	4.77	4.80	0.26	0.20
CsBr	4.22	4.26	0.25	0.19
CsI	3.54	3.57	0.23	0.19

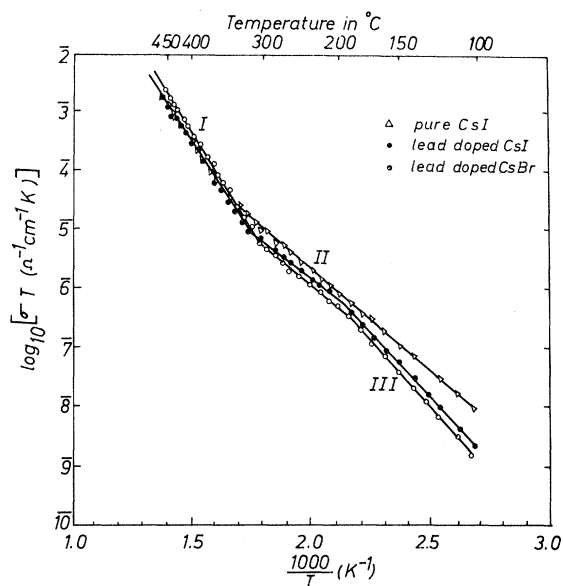


FIG. 5. Conductivity results for pure and Pb^{++} -doped cesium halides. Curve 1 shows the conductivity data for pure CsI. Curves 2 and 3 show the results for CsI and CsBr crystals containing 80 ppm of lead.

obtained in lead-doped cesium iodide and cesium bromide crystals. Curve 1 is for a pure CsI crystal and curves 2 and 3 are for CsI and CsBr crystals containing 80 ppm of lead impurity in the divalent state, respectively. It is evident from the figure that in the pure CsI crystal, two regions have been observed. To explain the results it is assumed that the primary charge carriers are anion vacancies while the divalent anion impurities (like CO_3^{2-} , SO_4^{2-} , etc.) are the dominant "background" impurities. On this basis the first region (I) in the conductivity plot for pure CsI can be considered as the region of intrinsic conductivity, whereas the second region (II), being governed by the concentration of "background" divalent anion impurities, gives the activation energy for the migration of the anion vacancies (created by the "background" impurities), which is roughly of the order of 0.4–0.5 eV. This value is large, which indicates that the effect of "background" divalent cation impurities can not be ignored. When divalent lead is added in CsI and CsBr, a third region (III) is also obtained as shown in Fig. 5. It is now evident that in the temperature range 100–350 °C the conductivity is dominated by the presence of divalent lead while above this temperature, it is intrinsic conductivity. On addition of divalent lead in the crystals, it is found that conductivity decreases in the extrinsic region in accordance with the earlier¹⁰ results. This decrease in conductivity is due to the decrease in the number of free anion vacancies by the law of mass action and conductivity is dominated by

cation vacancies created for the charge compensation which indicates that the conductivity is not anionic in nature at low temperatures. Thus regions II and III correspond to E_c and $E_c + \frac{1}{2}W_a$, respectively. From the conductivity results at higher temperatures and by using previous⁸ diffusion data (in order to get the contribution of anion vacancies), we have obtained a value for the formation energy of Schottky defects which agrees well with the previous results.⁸ The energy parameters obtained from conductivity measurements are tabulated in Table V.

2. Dielectric-Loss Measurements

In cesium halides each cesium ion is surrounded by six nearest-neighbor (nn) and twelve next-nearest-neighbor (nnn) cesium ions and the vacancies created on addition of divalent impurity can be situated in any of these sites. In the low-temperature region the vacancies form complexes with the impurity, owing to the electrostatic attraction, and such a complex has an electric dipole moment. External electric field would orient these defects preferentially, and removal of such a disturbing agency would tend to bring back the normal situation resulting in relaxation loss. The time taken for such a return would mainly depend on the radius of the impurity and host lattice symmetry. The relaxation time τ has been obtained theoretically^{21–23} as well as experimentally^{24–26} for alkali halides of fcc structure containing divalent impurities, but no such data exist for bcc lattices. In order to see the effect of change of host lattice symmetry on τ and to confirm the presence of lead in divalent form in cesium halides, dielectric-loss measurements have been performed on this system.

Typical results on the measurement of the dielectric-loss factor $\tan\delta$ are shown in Fig. 6. These results are obtained in the case of cesium iodide crystals containing 80 ppm of divalent lead and curves 1, 2, 3, 4, and 5 are the $\tan\delta$ versus frequency isothermals obtained at 100, 120, 140, 160, and 180 °C, respectively. Each curve shows only

TABLE V. Energy parameters for Pb^{++} -doped alkali halides of fcc and bcc structures obtained from conductivity results. W_s , energy of formation of Schottky defects; E_c , energy of migration of cation vacancies; W_a , free energy of association of the impurity ion and cation vacancies. All the energies are expressed in eV.

Crystal	W_s	E_c	W_a	Ref.
NaCl	2.24	0.78	0.28	3
KCl	2.14	0.78	0.26	3
KBr	1.84	0.68	0.27	3
KI	1.70	0.69	0.28	3
CsBr	1.86	0.64	0.48	This work
CsI	1.84	0.63	0.46	This work

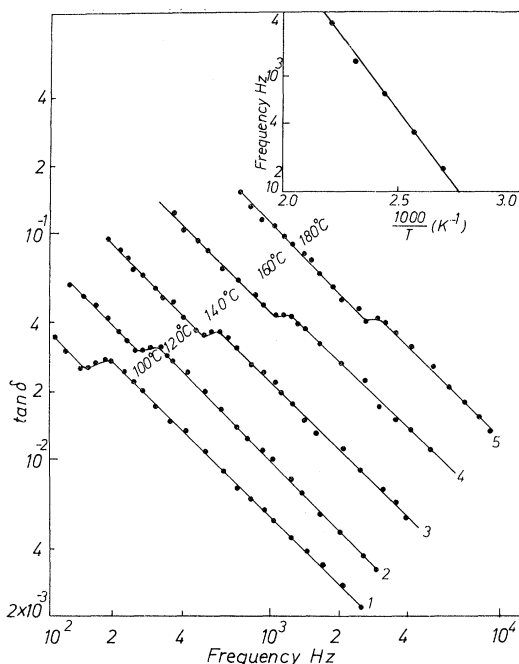


FIG. 6. Dielectric-loss results for CsI crystal containing 80 ppm of divalent lead. Curves 1, 2, 3, 4, and 5 are $\tan \delta$ vs frequency isothermals obtained at 100, 120, 140, 160, and 180 °C, respectively. Inset shows a straight-line plot of $\log_{10} f_m$ vs $1000/T$ for the determination of activation energy and frequency factor for lead-impurity-vacancy dipoles.

one loss peak and the peak frequency f_m of the loss peak shifts to the higher frequencies as the temperature is increased. The inset in Fig. 6 shows the plot of $\log_{10} f_m$ vs $1000/T$ where T is the temperature of measurement of dielectric-loss factor in K. Since the plot is a straight line, the peak frequency can be expressed as

$$f_m = f_0 e^{-E/kT}, \quad (4)$$

where f_0 is the preexponential factor and E is the activation energy for the jump of a cation vacancy bound to the impurity ion. The slope of the straight line gives the value of activation energy for the migration of a bound cation vacancy as 0.62 eV in CsI containing divalent lead. Measurements were performed with different concentrations of lead, and it is found that the position of peak frequencies remains the same in all the cases. Table VI shows a comparison of the behavior of lead-impurity-vacancy dipoles in different crystals.

In order to remove the possibility of aggregation of impurity-vacancy dipoles, the crystals have been given different heat treatments before being quenched to the desired temperature of the measurements. The results of dielectric-loss measurements show that the loss peak increases in magnitude for quenching temperature up to 300 °C.

This increase in the height of the loss peak indicates that at ordinary temperature a certain number of impurity-vacancy pairs exist as larger aggregates which dissociate into simple pairs when the crystal is heated to higher temperatures. The magnitude of the peak becomes constant on heating up to 300 °C, showing thereby that all the aggregates have been dissolved. Therefore, the final measurements are made on a crystal which is quenched from 300 °C. Measurements were also made on pure crystals under identical conditions which showed no relaxation losses; this rules out the possibility of background impurities playing any role in the present observations.

According to earlier work by Dreyfus,²⁴ if the radius of the impurity ion is considerably smaller than that of the host cation, one would expect two relaxation loss peaks, which can be ascribed to the jump of a vacancy in the nn and nnn sites. However, in the present work we observed only one loss peak, although the radii of Pb^{2+} (1.32 Å) and Cs^+ (1.67 Å) are different. As the radius of the impurity ion increases, the probability for the occupation of nnn sites by the vacancy decreases, and hence it will be difficult to observe relaxation loss due to the jump of vacancy in nnn sites. This may be a possible reason for the absence of a second peak in cesium halides containing the divalent lead ion. It may also be possible that in the case of bigger and heavy impurity ions embedded in bcc lattices, the theory may not be as applicable as it is in the case of smaller ions like Mn^{2+} , Co^{2+} , and Ni^{2+} doped in fcc lattices.²⁷⁻²⁹ Recent experiments²⁶ on the reorientation of the impurity-vacancy complexes in KCl containing divalent substitutional ions by the depolarization thermocurrent method also give results which are difficult to reconcile on the basis of the theory proposed by Dreyfus. Thus the single peak observed in the present case is attributed to the dipoles consisting of divalent lead and the nearest-neighbor cation vacancy. It is evident from Table VI that the values of E and f_0 are different from those obtained earlier⁴ for lead-doped fcc lattices, which indicates that the entropy of activation of a cation vacancy depends

TABLE VI. Activation energies and preexponential factor for the loss peak calculated from a straight-line plot of Fig. 6.

Crystal	E (eV)	f_0 (sec ⁻¹)	Ref.
KCl	0.78	1.3×10^{12}	4
KBr	0.69	5.0×10^{11}	4
KI	0.80	1.4×10^{15}	4
CsCl	0.64	5.2×10^{10}	This work
CsBr	0.65	8.83×10^{10}	This work
CsI	0.62	2.2×10^{10}	This work

both on the electronic configuration of the neighboring divalent impurity ion and on the host lattice symmetry.

IV. SUMMARY

Optical absorption, conductivity, and dielectric-loss measurements have been made on lead-doped cesium halides. Except for the few differences, the lead centers in cesium halides behave identical to those in alkali halides. The *A* band in lead-doped cesium halides exhibits a doublet structure, in contrast to the other lead-doped alkali halides, where the *A* band is of simple bell shape. The formation of Pb^+ and Pb^0 centers has been inferred from the radiation damage studies. The conduc-

tivity studies of Pb^{++} -doped cesium halides show the decrease of conductivity in the extrinsic region which has been explained by considering the plausible reasons. A single loss peak has been observed in the dielectric-loss measurements; that peak has been attributed to the jump of a vacancy to the nn position.

ACKNOWLEDGMENTS

The authors wish to express their sincere thanks to Professor C. J. Delbecq, Professor A. Fukuda, and Professor C. Ramasastry, who have given some valuable suggestions. We would also like to thank Dr. B. V. R. Chowdari and Dr. R. Thyagarajan for providing some pure crystals.

- ¹R. Hilsch, Z. Physik 44, 860 (1927).
²A. Fukuda, Sci. Light (Tokyo) 13, 64 (1964).
³S. C. Jain, S. Radhakrishna, and K. S. K. Sai, J. Phys. Soc. Japan 27, 1179 (1969).
⁴S. C. Jain, K. S. K. Sai, and K. Lal, J. Phys. C 4, 1958 (1971).
⁵J. P. Stott and J. H. Crawford, Jr., Phys. Rev. B 4, 439 (1971).
⁶D. Schoemaker and J. L. Kolopus, Solid State Commun. 8, 435 (1970).
⁷S. Masunaga, I. Morita, and M. Ishiguro, J. Phys. Soc. Japan 21, 638 (1966).
⁸D. W. Lynch, Phys. Rev. 118, 468 (1960).
⁹I. M. Hoodless and B. D. McNicols, Phil. Mag. 17, 1223 (1968).
¹⁰M. V. Pashkovskii, I. M. Spitkovskii, and A. D. Tkachuk, Fiz. Tverd. Tela 12, 1317 (1970) [Sov. Phys. Solid State 12, 1036 (1970)].
¹¹K. V. Reddy, Ph.D. thesis (I. I. T., Madras, 1972) (unpublished).
¹²F. Seitz, J. Chem. Phys. 6, 150 (1938).
¹³Y. Toyozawa and M. Inoue, J. Phys. Soc. Japan 21, 1663 (1966).
¹⁴A. Fukuda, J. Phys. Soc. Japan 27, 96 (1969).
¹⁵S. G. Zazubovich, Phys. Status Solidi 38, 119 (1970).
¹⁶S. Sugano, J. Chem. Phys. 36, 122 (1962).
¹⁷V. C. Sethi and A. M. Karguppikar, Phys. Status Solidi (b) 50, K63 (1972).
¹⁸J. H. Schulman, R. J. Ginter, and C. C. Klick, J. Opt. Soc. Am. 40, 854 (1950).
¹⁹W. A. Sibley, E. Sonder, and C. T. Butler, Phys. Rev. 136, A537 (1964).
²⁰A. B. Lidiard, in *Handbuch der Physik* (Springer, Berlin, 1957), Vol. 20, p. 246.
²¹A. B. Lidiard, in Report of the Conference on Defects in Crystalline Solids, Bristol, 1954, p. 261 (unpublished).
²²S. Radhakrishna, J. Phys. C 1, 644 (1968).
²³P. V. Pantulu and S. Radhakrishna, Proc. Ind. Acad. Sci. 67, 109 (1968).
²⁴R. W. Dreyfus, Phys. Rev. 121, 1675 (1961).
²⁵C. Bucci and R. Fieschi, Phys. Rev. Letters 12, 16 (1964).
²⁶A. Brun, P. Dansas, and F. Sixou, Solid State Commun. 8, 613 (1970).
²⁷G. D. Watkins, Phys. Rev. 113, 91 (1959).
²⁸S. C. Jain and K. Lal, Proc. Phys. Soc. (London) 92, 990 (1967).
²⁹K. Lal and D. R. Pahwa, Phys. Rev. B 4, 2741 (1971).